

# ビジュアルリフティングアプローチによる二足歩行の安定性解析

○神 克礼 李 想 田 宏志 井澤 大時 見浪 護 松野 隆幸 (岡山大学)

## Stability Analyses of Biped-walking by Visual-lifting Approach

\*Keli Shen, Xiang Li, Hongzhi Tian, Daiji Izawa, Mamoru Minami and Takayuki Matsuno  
(Okayama University)

**Abstract**– Biped walking control has been realized by Zero-Moment Point (ZMP). The efficiency of ZMP was well verified in keeping stable walking, but ZMP based walking cannot stop falling. Besides, dynamical walking can be used for walking that realizes kicks by toes, which does not depend on ZMP. Though the dynamical walking seems to be natural, robots tend to fall. Therefore, it is necessary for realization of human-like walking to keep dynamical walking stable. In our research, we have proposed a dynamical equation for walking derived by the Newton-Euler method including slipping, impact, line-touch and surface-touch of the foot. “Visual Lifting Approach” (VLA) is equipped to enhance the walking stability and stops the biped robot from falling without using ZMP. The VLA includes visual-lifting feedback and feedforward of walking gait generation. In this paper, we discuss how to realize the stable walking according to some measurements such as angle of ankle of floating foot, Center of Gravity (COG), waist angular velocity, height of head and waist and walking step length.

**Key Words:** Humanoid, Biped-walking, Visual-lifting Approach, Feedforward Inputs, Stability

## 1 Introduction

In many biped-walking control strategies of the humanoid, ZMP-based walking motion is considered as most efficient method, which has been certified to be useful in keeping stability of practical biped-walking, since it can make sure that humanoid robots can keep the balance of walking and standing by retaining the ZMP within the convex hull of supporting area<sup>1, 2)</sup>. However, ZMP control makes the humanoid robots' waist lower and look like monkey while walking. Besides, other methods except ZMP are proposed to concentrate on keeping the biped-walking trajectories in side of a basin of attraction<sup>3, 4, 5)</sup>, including a way referring limit cycle to determining input torque<sup>6)</sup>.

These previous methods discussed are based on simplified biped models, which try to avoid discussing the effects of feet or slipping existing in real environment, Different from the above reference, one study<sup>7)</sup> has pointed out the effect of foot having many walking gaits such as surface contacting (foot sole contacting with ground) and point contacting (heel contacting), changing the dimension of state variables. Our research has started from view point of<sup>7)</sup> to describe the dynamics of gaits including point/surface-contacting state of foot, slipping of the foot and bumping as correctly as possible. It is called event-driven where walking gait transition would be determined by the past walking motion. The model in<sup>7)</sup> only has foot model different from our model including the dynamics of whole-body humanoid with arms and head. And what the authors want to point out is that the dimension of equation of motion is changed by the varieties of the biped-walking introduced in<sup>8)</sup> concerning one-legged hopping robot.

If the heel is detached from ground while its toe is contacting, a new state variable describing the rota-

tion of foot will emerge, increasing the number of state variables. In fact, this kind of dynamics with dimension number of state variables changed by the result of its dynamical time profiles of motions are out of the area of control theory discussing how to control a system with fixed states' number. Further the tipping over motion has been called non-holonomic dynamics including a joint such as free joint without inputting torque.

At the same time, the heel or the toe of lifting foot in the air contacts with the ground geometrically. The referred paper<sup>9)</sup> discussed the method of representing contacting with environment dealing constraint motion with friction by algebraic equation and applied it to human configuration<sup>10)</sup>. According to these references, dynamics of 20 kinds of gaits were derived including slipping motion with both different constraint conditions and change of the dimension of state variables where the humanoid's dynamical model has been sufficient as much as possible<sup>11)</sup>.

In previous research on VLA in<sup>12, 13, 14)</sup>, the incomplete model of humanoid was applied in which head, arms and torso were neglected. Thus, there are some drawbacks, i.e., the model was too simple to consider the effect of dynamical coupling of arm and upper body. However, the new model proposed in this paper has been optimized concerning the above problem, and the discussion of slipping and effectiveness of the model have been proved in<sup>11)</sup>.

In this paper, Visual-lifting Approach(VLA) based on visual servo and visual feedback concept is examined to realize the human-like natural walking with slippage including toe-off state. Real-time position and orientation tracking method to observe a 3D object that is put near the humanoid to measure the robot's head relative pose has been proposed as visual pose estimation<sup>15, 16)</sup>. The simulation result in-

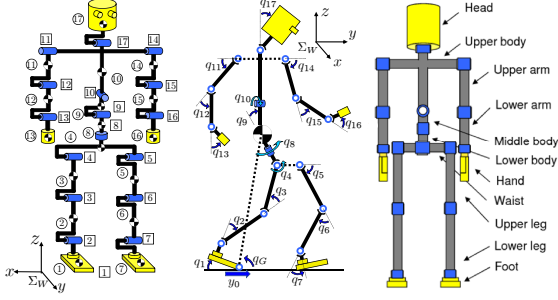


Fig. 1: Definition of biped-walking model, ①~⑰ represents link number, [1]~[17] is joint number,  $q_1 \sim q_{17}$  is joint angles.

Table 1: Physical parameters

Link	$l_i$ [m]	$m_i$ [kg]	$d_i$ [Nms/rad]
Head	0.24	4.5	0.5
Upper body	0.41	21.5	10.0
Middle body	0.1	2.0	10.0
Lower body	0.1	2.0	10.0
Upper arm	0.31	2.3	0.03
Lower arm	0.24	1.4	1.0
Hand	0.18	0.4	2.0
Waist	0.27	2.0	10.0
Upper leg	0.38	7.3	10.0
Lower leg	0.40	3.4	10.0
Foot	0.07	1.3	10.0
Total weight [kg]	—	64.2	—
Total hight [m]	1.7	—	—

indicates that visual feedback control and feedforward inputs are useful to realize the stable biped-walking on the condition that humanoid's dynamics includes toe-off, slipping and bumping. Besides, this paper discuss how to realize the stable walking according to some measurements such as angle of ankle of floating foot, Center of Gravity (COG), waist angular velocity, height of head and waist and walking step length.

## 2 Biped-walking Model

The biped-walking robot in Fig.1 is discussed in this paper, Table 1 shows length  $l_i$  [m], mass  $m_i$  [kg] of links and coefficient of joints' viscous friction  $d_i$  [N·m·s/rad], which are determined by<sup>17)</sup>. This model is simulated as a serial-link manipulator having branches and represents rigid whole-body such as feet including toe, torso, arms and so on and is up to 17 degree-of-freedom. Though motion of legs is limited in sagittal plane, it generates many walking gaits since the robot has flat-sole feet and kicking torque. In this paper, the foot named as link-1 is defined as "supporting-foot" and the other foot named as link-7 is defined as "free-foot" ("contacting-foot" when the free-foot contacts with ground) based on gaits. When the contacting-foot stopped slipping which indicated that static friction force is exerted to the foot, the contacting-foot is transferred into supporting-foot

and the previous supporting-foot is changed to free-foot if it was isolated from floor.

## 3 Dynamical Calculations and Analyses

Equation of motion with one foot standing can be donated,

$$M(\mathbf{q})\ddot{\mathbf{q}} + \mathbf{h}(\mathbf{q}, \dot{\mathbf{q}}) + \mathbf{g}(\mathbf{q}) + \mathbf{D}\dot{\mathbf{q}} = \boldsymbol{\tau}, \quad (1)$$

Here,  $\boldsymbol{\tau} = [f_{y_0}, \tau_1, \tau_2, \dots, \tau_{17}]$  is input torque, where  $f_{y_0}$  is always zero since the slipping motion has no actuators.  $M(\mathbf{q})$  is inertia matrix,  $\mathbf{h}(\mathbf{q}, \dot{\mathbf{q}})$  is the vector indicating Coriolis force and centrifugal one, and  $\mathbf{g}(\mathbf{q})$  is gravity one. The  $\mu_k$  in  $\mathbf{D} = \text{diag}[\mu_k, d_1, d_2, \dots, d_{17}]$  represents coefficient of friction,  $\mu_k$  is the one between foot and ground. And  $\mathbf{q} = [y_0, q_1, q_2, \dots, q_{17}]^T$  includes the relative position between foot and ground  $y_0$  generated by slipping and the angle of joints  $q_1 \sim q_{17}$ .

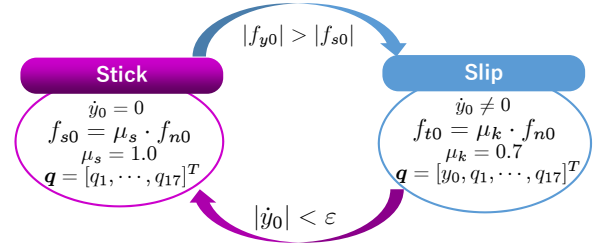


Fig. 2: Switch conditions of stick-slip motion

This stick motion state is described at left side of Fig.2. If  $|\dot{y}_0| < \epsilon$  is satisfied, the degree of motion  $y_0$  will disappear and the equation of motion will transfer to the equation of motion consisting of  $\mathbf{q} = [q_1, q_2, \dots, q_{17}]^T$ . On this state, static friction coefficient  $\mu_s = 1.0$  is employed, and static friction force  $f_{s0} = \mu_s f_{n0}$  exerts to the lateral direction of foot.

However, when the supporting-foot (1-st link) is slipping (prismatic joint), the force exerting onto the 1-st link can be calculated by following equation.

$$f_{y_0} = e_{z_0}^T \mathbf{f}_0 + \mu_k \dot{y}_0. \quad (2)$$

where  $\dot{y}_0$  is slipping velocity. The viscous friction force of  $y$ -axis (slipping axis) described as  $\mu_k \dot{y}_0$  is shown in left-hand side of Eq.(2).

If the exerting lateral force  $f_{y_0}$  generated by dynamical coupling of humanoid body calculated by Eq.(2) satisfies  $|f_{y_0}| > |f_{s0}|$ , the slipping motion will start and the equation of motion, Eq.(2), will be changed into the one with variables of  $\mathbf{q} = [y_0, q_1, q_2, \dots, q_{17}]^T$  again, which is shown at the right state Fig.2.

## 4 Visual-lifting Approach

### 4.0.1 Feedback-lifting Torque Generator

This section proposes a visual-lifting feedback to improve biped standing/walking stability as shown in Fig.3. We apply a model-based matching method to

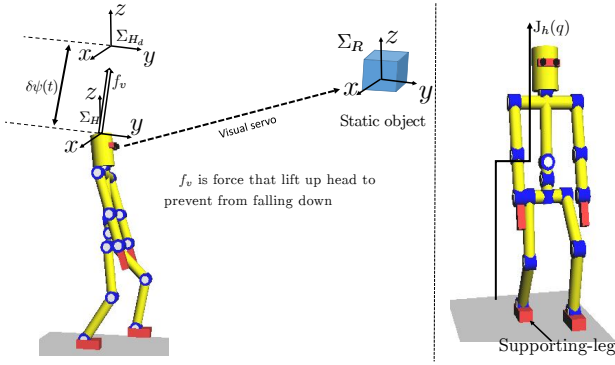


Fig. 3: Concept of Visual Lifting Stabilization.

evaluate posture of a static target object described by  $\psi(t)$  representing the robot's head based on  $\Sigma_H$ . The relatively desired posture of  $\Sigma_R$  (coordinate of reference target object) and  $\Sigma_H$  is predefined by Homogeneous Transformation as  ${}^H\mathbf{T}_R$ . The difference of the desired head posture  $\Sigma_{H_d}$  and the current posture  $\Sigma_H$  is defined as  ${}^H\mathbf{T}_{H_d}$ , it can be described by:

$${}^H\mathbf{T}_{H_d}(\psi_d(t), \psi(t)) = {}^H\mathbf{T}_R(\psi(t)) \cdot {}^{H_d}\mathbf{T}_R^{-1}(\psi_d(t)), \quad (3)$$

where  ${}^H\mathbf{T}_R$  is calculated by  $\psi(t)$ .  $\psi(t)$  can be measured by on-line visual posture evaluation proposed by <sup>15, 16</sup>. However, we assume that this parameter is set directly. Here, the force is considered to be directly proportional to  $\delta\psi(t)$ , which is exerted on the head to minimize  $\delta\psi(t) = \psi_d(t) - \psi(t)$  calculated from  ${}^H\mathbf{T}_{H_d}$ . The deviation of the robot's head posture is caused by gravity force and the influence of walking dynamics. The joint torque  $\tau_h(t)$  lifting the robot's head is donated:

$$\tau_h(t) = \mathbf{J}_h(\mathbf{q})^T \mathbf{K}_p \delta\psi(t), \quad (4)$$

where  $\mathbf{J}_h(\mathbf{q})$  in Fig.3 is Jacobian matrix of the head posture against joint angles including  $q_1, q_2, q_3, q_4, q_8, q_9, q_{10}, q_{11}, q_{17}$ , and  $\mathbf{K}_p$  is proportional gain like impedance control. We apply this input to stop falling down caused by gravity or dangerous slipping gaits happened unpredictably during walking progress. We stress that the input torque for non-holonomic joint such as joint-1,  $\tau_{h_1}$  in  $\tau_h(t)$  in (4) is zero for its free joint.  $\delta\psi(t)$  can show the deviation of the humanoid's position and orientation, however, only position is discussed in this study.

#### 4.0.2 Foot and Body Motion Generator

Besides  $\tau_h(t)$ , in order to make the floating-foot and supporting-foot step forward, added input torques  $\tau_t(t) = [0, \tau_{t2}, \tau_{t3}, 0, \tau_{t5}, \tau_{t6}, \tau_{t7}, 0, \dots, 0]^T$  are used. And another kind of input torques  $\tau_w(t) = [0, \dots, 0, \tau_{w8}, 0, \dots, 0]^T$  is used to swing the roll angle of the waist (joint-8), which further realizes the arm swinging motion through dynamical coupling. Here,  $\tau_t(t)$  and  $\tau_w(t)$  are seen as feed-forward input torques. Here,  $t_2$  means the time that supporting-foot

and contacting-foot are switched. The elements  $\tau_t(t)$  and  $\tau_w(t)$  are shown below:

$$\tau_{t5} = \begin{cases} 20\cos(2\pi(t - t_2)/1.45), & (t < 1.0[s]) \\ 15\cos(2\pi(t - t_2)/1.85), & (t \geq 1.0[s]), \end{cases} \quad (5)$$

$$\tau_{w8} = \begin{cases} 50\sin 2\pi(t - t_2)/1.85, & (\text{right foot is supporting}) \\ -50\sin 2\pi(t - t_2)/1.85, & (\text{left foot is supporting}). \end{cases} \quad (6)$$

When time  $t < 1.5[s]$ ,  $\tau_{t2}, \tau_{t3}, \tau_{t6}, \tau_{t7}$  are set as feedback inputs.

$$\tau_{t2} = 40(-0.2 - q_2), \quad (7)$$

$$\tau_{t3} = 50(0.3 - q_3), \quad (8)$$

$$\tau_{t6} = 100(-0.4 - q_6). \quad (9)$$

$$\tau_{t7} = \begin{cases} 60(0.6 - q_7), & (\text{the first step}) \\ 20(0.35 - q_7), & (\text{others}). \end{cases} \quad (10)$$

When time  $t > 1.5[s]$ ,  $\tau_{t2}, \tau_{t3}, \tau_{t6}, \tau_{t7}$  are set as feed-forward inputs.

$$\tau_{t2} = 10\sin(2\pi(t - t_2)), \quad (11)$$

$$\tau_{t3} = -10 + 10\sin(2\pi(t - t_2)), \quad (12)$$

$$\tau_{t6} = -20 + 20\sin(\pi(t - t_2)). \quad (13)$$

$$\tau_{t7} = \begin{cases} 60, & (\text{floating and } q_7 \leq 0.6[\text{rad}]) \\ -40, & (\text{point-contacting and } q_7 \geq 0.35[\text{rad}]) \\ 0, & (\text{in other cases}). \end{cases} \quad (14)$$

#### 4.1 Combined lifting/swinging controller

Combining three torque generators in Eqs.(4)~(14), the controller for walking is derived,

$$\tau(t) = \tau_h(t) + \tau_t(t) + \tau_w(t). \quad (15)$$

## 5 Simulation of biped-walking by VLA

In the environment that sampling time was set to  $2.0 \times 10^{-4}[s]$  and coefficient of friction between the foot and the ground was set to  $\mu_s = 1.0$  (static friction coefficient),  $\mu_k = 0.7$  (viscous friction coefficient), the following simulation experiments were carried out. The desired position of head is set to  $\psi_d = [0, 0, 2.30[m]]$ . Concerning simulation environment, we used "Borland C++ Builder Professional Ver. 5.0" to make simulation program and "OpenGL Ver. 1.5.0" to display humanoid's time-transient configurations.

In this section, some figures are obtained to analyze the stability of biped-walking in the simulation. In this simulation, we set lifting proportional gain  $\mathbf{K}_p = \text{diag}[20, 290, 1010]$ .

In Fig.4, X-axis represents the walking time, Y-axis represents the step length of walking. Biped walking includes three phases: initial phase, transient phase



Fig. 4: Step length of Biped walking during 21 steps.

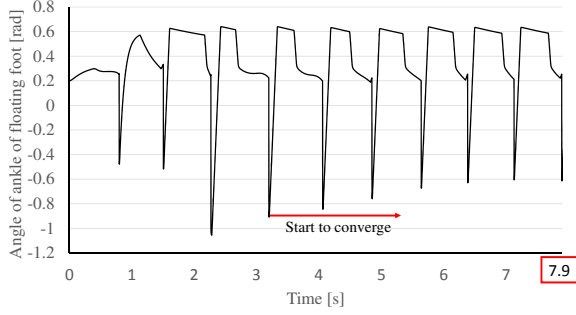


Fig. 5: Angle  $q_7$  of ankle joint of floating foot (from the 1st step to the 11th step).

and stable walking phase. From Fig.4, the step length comes to convergence after 5th step. And biped robot walks as the same step length 0.5[m] after finishing 11th step.

Figures 5 and 6 show the change of the angle of ankle of the floating foot. Fig.5 shows that the angle of floating foot change irregularly before the 11th step. X-axis represents the time, Y-axis represents the angle of ankle joint of the floating foot. From this figure, the change shape of angle is different. After the 5th step, the change shape of angle starts to converge. After 11th step (after 8.69[s]), the angle of ankle of floating foot change regularly in the certain range and Gait Cycle (time of finishing one step walking) changes in the limited range (from 0.77[s] to 0.79[s]), which indicates that the gaits of floating foot change periodically. From the figure, the shape change of angle is similar from one step to another. The walking motion becomes stable after 11th step.

Figure 7 show the Center Of Gravity(COG) position during 100 step simulation. The upper part of Fig.7 shows the screen shot of the biped walking simulation. The point A means the initial posture. B and B' show the state before and after the switching of supporting foot in the 1st step. The points of C and C' show the second time of supporting foot switching. The lower two columns show the transition of position of COG from initial phase and transient phase to stable phase, which are depicted by coordinate  $\Sigma_{toe}$  that is fixed at the toe of the supporting foot. Fig.7 (b), (c)

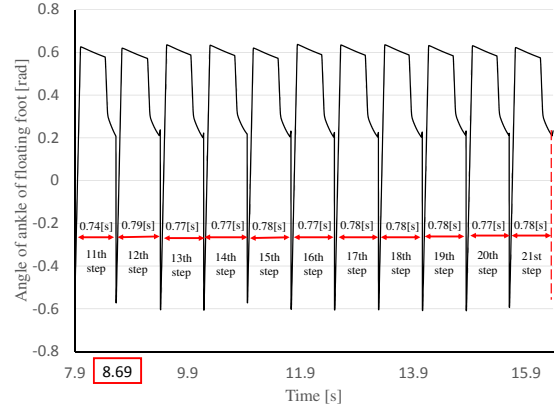


Fig. 6: Angle  $q_7$  of ankle joint of floating foot (after 11th step).

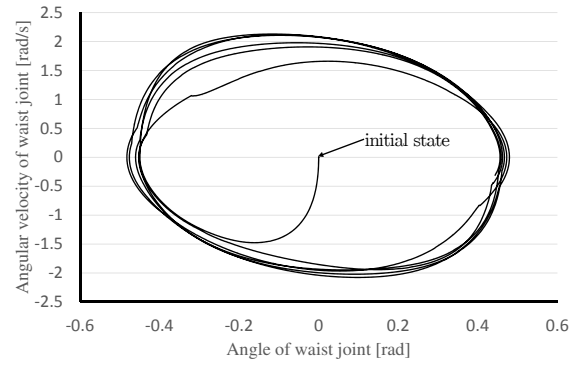
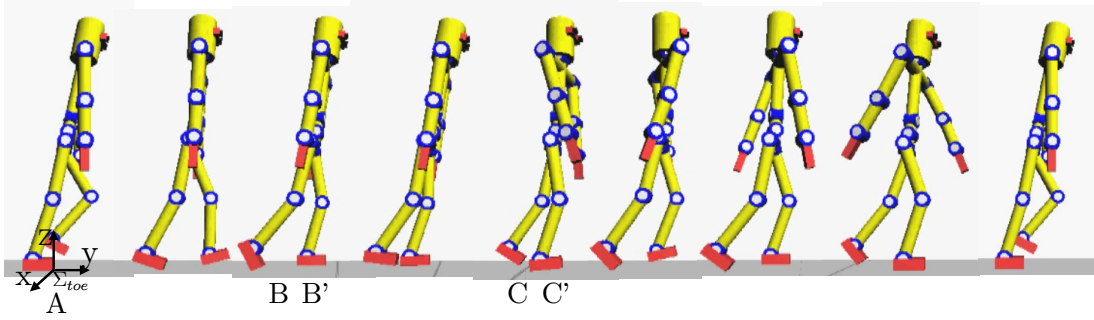


Fig. 8: Relation of angle  $q_8$  and angular velocity  $\dot{q}_8$  of waist joint in initial stage and convergence stage (from the 1st step to the 11th step).

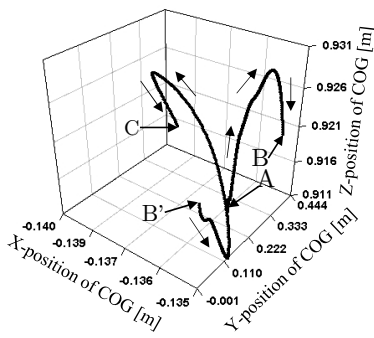
and (d) shows the initial phase and transient phase, the trajectory is complexed and no obvious similarity. In these figures, the position profile with A, B, B', C, C' corresponding to them in screen shots in Fig.7 (a). After entering stable walking shown in Fig.7 (e), (f) and (g), the trajectory of COG is converge to specific tendency, which is similar and along a narrow trajectory ( the width of trajectory is less than 0.002[m]).

Figure 8 and 9 represent the relation of angle  $q_8$  and angular velocity  $\dot{q}_8$  of waist joint during 100 steps. It is related to the stability of walking. Fig.8 shows the initial phase and transient phase (from 1st step to 11th step). In this phase, the movement of the waist includes varieties and does not converge to one trajectory. When entering the stable state shown in Fig.9, the movement of the waist enters a limit cycle with a very small width.

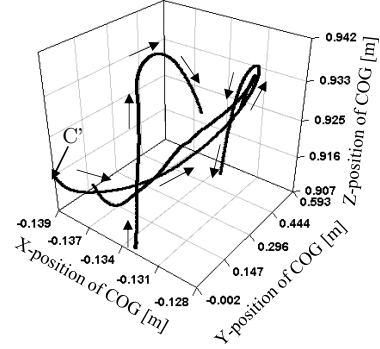
Figure 10 and 11 show the Z-axis position of head and waist based on the world coordinate system  $\Sigma_w$  during 100 steps walking. Fig.10 shows that the movement of both of head and waist has steady oscillations, which can be seen that the trajectory of motion is stable. Fig.11 is the expansion of Fig.10 in time. the height of head and waist before entering the stable state is described more obviously than Fig.10. Be-



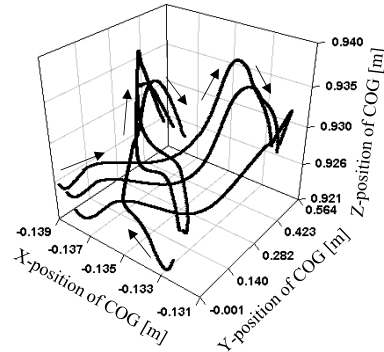
(a) Screen-shot of the biped-walking



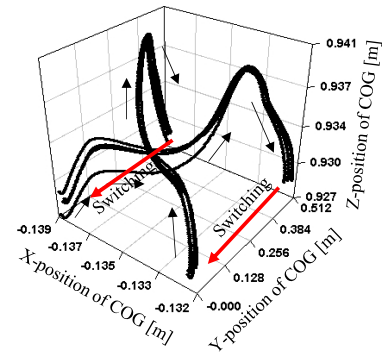
(b) COG position of 1st~2nd step



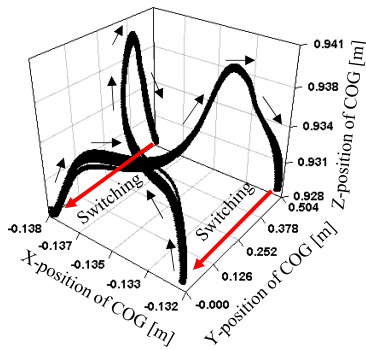
(c) COG position of 3rd~5th step



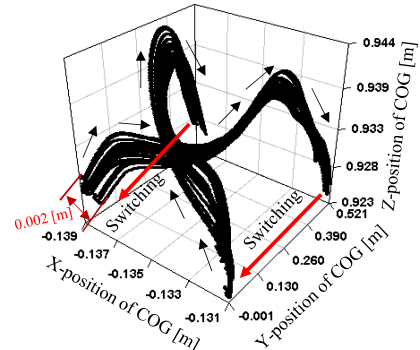
(d) COG position of 6th~11th step



(e) COG position of 12th~21st step



(f) COG position of 22nd~50th step



(g) COG position of 51st~100th step

Fig. 7: COG position during 100 steps walking simulation. The point of A means the initial posture, B and B' represent the state before and after the switching of supporting-foot in the first step. The C and C' show the second time of supporting foot switching. There are three states in the walking simulation. From 1st step to 5th step is the initial state, and from 6th step to 11th step is the transient state, after 11th step is the stable state.

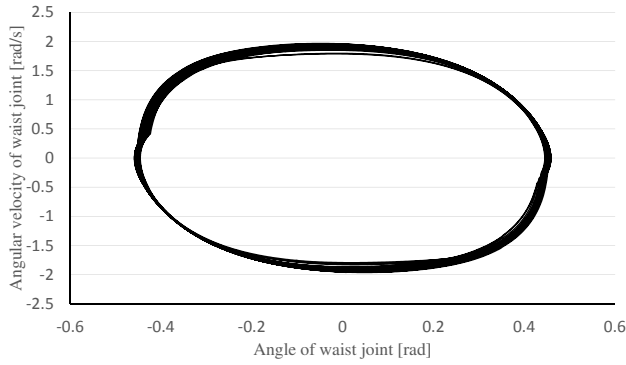


Fig. 9: Relation of angle  $q_8$  and angular velocity  $\dot{q}_8$  of waist joint in stable stage (after the 11th step).

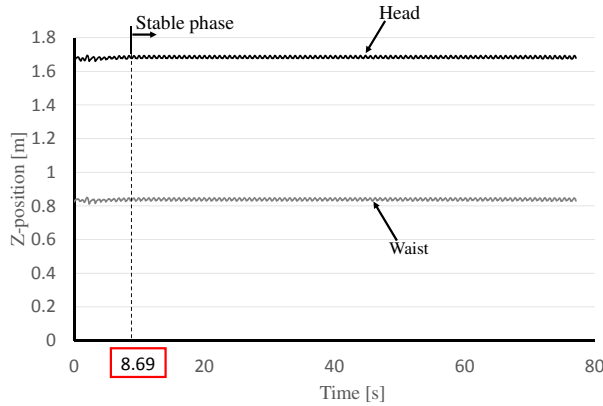


Fig. 10: Z-axis position (height) of head and waist joint based on the world coordinate system  $\Sigma_w$  during 100 steps walking. After the 11th step, the walking state is stable.

fore the 11th step, the height difference of waist and head is  $0.03[m]$ . After 11th step, difference becomes smaller and changes regularly. Therefore, the vibrational motion of head and waist become stable.

## 6 Conclusion

In this paper, the stability of walking is proved by some measurements such as step length, angle of ankle of floating foot and COG, waist angular velocity, height of head and waist. The results show Visual Feedback Control and Feedforward inputs based on the dynamical model that contains flat feet including toe, slipping and impact are effective to realize the stable walking, which is human-like natural walking. In the future work, we will adjust visual lifting gains to shorten the transient time and observe the versatility of feedforward inputs.

## Reference

- 1) M. Vukobratovic, A. Frank and D. Juricic: On the Stability of Biped Locomotion, IEEE Transactions on Biomedical Engineering, Vol.17, No.1 (1970)
- 2) M. Vukobratovic and J. Stepanenko: On the Stability of Anthropomorphic Systems, Mathematical Biosciences, Vol.15, pp.1/37 (1972)
- 3) S. Collins, A. Ruina, R. Tedrake and M. Wisse: Efficient Bipedal Robots Based on Passive-Dynamic

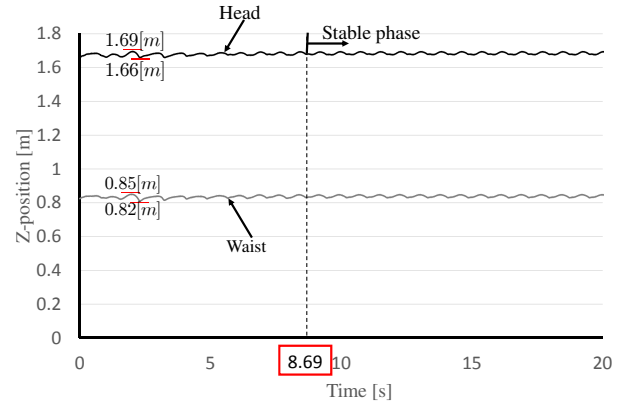


Fig. 11: Z-axis position (height) of head, waist joint before the stable state in Fig.10. After the 11th step, the vibrational motion of head and waist becomes steady

- Walkers, Science, Vol.307, pp.1082/1085 (2005)
- 4) J. Pratt, P. Dilworth and G. Pratt: Virtual Model Control of a Bipedal Walking Robot, Proceedings of IEEE International Conference on Robotics and Automation, pp.193/198 (1997)
- 5) R.E. Westervelt, W.J. Grizzle and E.D. Koditschek: Hybrid Zero Dynamics of Planar Biped Walkers, IEEE Transactions on Automatic Control, Vol.48, No.1, pp.42/56 (2003)
- 6) Y. Harada, J. Takahashi, D. Nenchev and D. Sato: Limit Cycle Based Walk of a Powered 7DOF 3D Biped with Flat Feet, Proceedings of IEEE/RSJ International Conference on Intelligent Robots and Systems, pp.3623/3628 (2010)
- 7) Y. Huang, B. Chen, Q. Wang, K. Wei and L. Wang: Energetic efficiency and stability of dynamic bipedal walking gaits with different step lengths, Proceedings of IEEE/RSJ International Conference on Intelligent Robots and Systems, pp.4077/4082 (2010)
- 8) T. Wu, T. Yeh and B. Hsu: Trajectory Planning of a One-Legged Robot Performing Stable Hop, Proceedings of IEEE/RSJ International Conference on Intelligent Robots and Systems, pp.4922/4927 (2010)
- 9) Y. Nakamura and K. Yamane: Dynamics of Kinematic Chains with Discontinuous Changes of Constraints—Application to Human Figures that Move in Contact with the Environments—, Journal of RSJ, Vol.18, No.3, pp.435/443 (2000)
- 10) K.Yamane and Y.Nakamura: Dynamics Filter - Concept and Implementation of On-Line Motion Generator for Human Figures, IEEE Transactions on Robotics and Automation, vol.19, No.3, pp.421/432 (2003)
- 11) Xiang Li, Hiroki Imanishi, mamoru Minami, Takayuki Matsuno, Akira Yanou: Dynamical Model of Walking Transition Considering Nonlinear Friction with Floor, Journal of Advanced Computational Intelligence and Intelligent Informatics, Vol.20 No.6 (2016)
- 12) Wei Song, Mamoru Minami and Yanan Zhang: A Visual Lifting Approach for Dynamic Bipedal Walking, International Journal of Advanced Robotic Systems, Vol.9, pp.1-8 (2012)
- 13) Akira Yanou, Mamoru Minami, Tomohide Maeba and Yosuke Kobayashi: A First Step of Humanoid's Walking by Two Degree-of-freedom Generalized Predictive Control Combined with Visual Lifting Stabilization, Proceedings of the 39th Annual Conference of the IEEE Industrial Electronics Society (IECON2013), pp.6357/6362 (2013)

- 14) Wei Song, Mamoru Minami, Tomohide Maeba, Yanan Zhang and Akira Yanou: Visual Lifting Stabilization of Dynamic Bipedal Walking, Proceedings of 2011 IEEE-RAS International Conference on Humanoid Robots, pp.345/351 (2011)
- 15) W. Song, M. Minami, F. Yu, Y. Zhang and A. Yanou: 3-D Hand & Eye-Vergence Approaching Visual Servoing with Lyapunov-Stable Pose Tracking, Proceedings of IEEE International Conference on Robotics and Automation, pp.5210/5217 (2011)
- 16) F. Yu, W. Song and M. Minami: Visual Servoing with Quick Eye-Vergence to Enhance Trackability and Stability, Proceedings of IEEE/RSJ International Conference on Intelligent Robots and Systems, pp.6228/6233 (2010)
- 17) M. Kouchi, M. Mochimaru, H. Iwasawa and S. Mitani: Anthropometric database for Japanese Population 1997-98, Japanese Industrial Standards Center (AIST, MITI) (2000)
- 18) T. Maeba, M. Minami, A. Yanou and J. Nishiguchi: Dynamical Analyses of Humanoid's Walking by Visual Lifting Stabilization Based on Event-driven State Transition, 2012 IEEE/ASME Int. Conf. on Advanced Intelligent Mechatronics Proc, pp.7/14 (2012)